Hot Purge Gas Regeneration of Adsorption Beds with Solute Condensation: Experimental Studies

Activated carbon beds with adsorbed *n*-octane are regenerated using hot air. Effects of pressure, feed temperature, and initial loading on temperature and concentration breakthrough curves are studied. For moderate and high values of these variables, effluent vapors are found to be saturated with hydrocarbon during part of the heating step, indicating the presence of liquid within the bed. Regeneration behavior is predicted with reasonable accuracy using a nonisothermal stage model.

D. K. FRIDAY and M. D. LeVAN

Department of Chemical Engineering
University of Virginia
Charlottesville, VA 22901

SCOPE

Cyclic adsorption systems used for solvent recovery, dehydration, and some bulk separations rely on *in situ* thermal regeneration to remove the adsorbate from the adsorbent. This is accomplished by passing either a hot purge gas or steam into the bed.

There are few published experimental studies of hot purge gas regeneration for which the phase equilibria relation is known. We have discussed elsewhere (Friday and LeVan, 1982, 1984) much of the previous work on nonisothermal adsorption and desorption, including the drying of fibers and agricultural products, for which temperature variations are mild. Of more immediate relevance to our work is the experimental study by Basmadjian et al. (1975) in which carbon dioxide and ethane were desorbed from activated carbon beds using hot purge gas. Measurements of concentration and temperature breakthrough curves compared favorably with predictions of an adiabatic model. Jacob and Tondeur (1983) have made similar comparisons for pentanes adsorbed on 5A molecular sieve.

Friday and LeVan (1982, 1984) have carried out modeling studies which show that a liquid phase can be developed in and passed through a fixed-bed adsorber during thermal regeneration with hot purge gas, and that increases in initial loading of the adsorbent, the regeneration pressure, and the regeneration feed temperature should increase the likelihood that the liquid phase is formed. Basmadjian (1984) has investigated the role that transfer resistances may play on water condensation in gas dehydration beds and has also found that the formation of a liquid phase should be favored by high regenerant temperature and pressure.

This paper reports experimental work on hot purge gas regeneration with emphasis on the condensation phenomenon. Results are obtained for the regeneration of a fixed-bed of Calgon type BPL activated carbon with adsorbed *n*-octane using hot air. Pressure, feed temperature, and initial loading of the adsorbate are treated as variables. Adsorption isotherm data are also measured, correlated, and used to predict regeneration behavior for comparison with observations.

The mathematical model used here to interpret breakthrough behavior is a nonisothermal stage model. We are concerned principally with factors that determine the heights of plateaus and the general shapes (abrupt and gradual) and locations of transitions, namely, material balances, the energy balance including heat losses, and phase equilibria relations. The stage model, closely related to the plate theory of chromatography, permits simple treatment of these factors. We do not treat in any detail mass and heat transfer resistances, dispersion, and deviations from plug flow (channeling), which, for a deep bed, affect only the detailed shapes of transitions.

CONCLUSIONS AND SIGNIFICANCE

This paper provides experimental evidence that a liquid phase can be formed within an adsorption bed during thermal regeneration with hot purge gas, even under mild conditions. Furthermore, it shows that if liquid is formed for a given set of conditions, a decrease in initial loading of the adsorbent, regeneration pressure, or regeneration feed temperature may prevent its formation.

Our experimental results can be described with reasonable accuracy by the simple nonisothermal stage model. The prediction of the development or lack of development of the saturated phase is in agreement with experimental results in all cases. Locations and general shapes of transitions and heights of plateaus are found to within experimental accuracy.

The development of the liquid phase is desirable in certain circumstances and should be avoided if possible in others. With the adsorbate removed from a column as saturated vapor, re-

Correspondence concerning this paper should be addressed to M. D. LeVan.
D. K. Friday is presently at Westvaco Corp., Laurel Research Center, Laurel, MD 20707.

covery by condensation is efficient. However, the development of liquid may lead to poor flow distribution of the purge gas, especially with upflow regeneration, and may affect the stability of some adsorbents.

MATHEMATICAL MODEL

A wide variety of approaches have been taken to fixed-bed adsorption modeling. Both distributed- and lumped-parameter models are now common. Because of the complexity of the problem considered here (see the Discussion section below), we have opted for a simple mathematical description of the regeneration process. The model differs from the one used by Friday and LeVan (1982) principally in that heat losses from the bed through the column wall are accounted for.

The appropriate conservation equations can be written

$$\rho_b \frac{\partial q}{\partial t} + \frac{\partial\{[(1-\epsilon)\chi + \epsilon]c\}}{\partial t} + \frac{\partial(\epsilon v c)}{\partial z} = 0 \tag{1}$$

$$\rho_b \frac{\partial h_s}{\partial t} + \frac{\partial\{[(1-\epsilon)\chi + \epsilon]\rho_f h_f\}}{\partial t} + \frac{\partial(\epsilon v \rho_f h_f)}{\partial z} = -\frac{2U\Delta T}{r_i} \tag{2}$$

where stationary-phase and fluid-phase enthalpies are defined by

$$h_s \equiv (c_s + c_a q)(T - T_{\text{ref}}) - \int_0^q \lambda\, dq \tag{3}$$

$$h_f \equiv c_f(T - T_{\text{ref}}) \tag{4}$$

Any liquid present is considered to be stationary. The overall heat transfer coefficient U, based on the inside surface area of the column, multiplies ΔT, the difference between local bed temperature and ambient temperature. The specific heat capacity of the stationary phase, c_s, is considered to include not only the heat capacity of the adsorbent but also effective heat capacities of the column wall and insulation. The latent heat of desorption or vaporization appearing in Eq. 1 is dependent on loading and is evaluated at the reference temperature.

Equations 1 and 2 can be simplified and written in terms of dimensionless independent variables. In adsorption operations involving vapors at low and moderate pressures, rates of accumulation of material and energy in the vapor phase are generally small compared to those for the stationary phase. Therefore, the second terms in Eqs. 1 and 2 may be discarded. The following dimensionless variables can be defined

$$\tau \equiv \frac{\epsilon_o v_o t}{L} \quad \zeta \equiv \frac{z}{L} \quad v^* \equiv \frac{\epsilon v}{\epsilon_o v_o} \tag{5-7}$$

The dimensionless time τ is equal to the number of bed volumes of hot regeneration gas that have been passed into the bed, based on an open column. Substituting these variables into Eqs. 1 and 2 gives

$$\rho_b \frac{\partial q}{\partial \tau} + \frac{\partial(v^* c)}{\partial \zeta} = 0 \tag{8}$$

$$\rho_b \frac{\partial h_s}{\partial \tau} + \frac{\partial(v^* \rho_f h_f)}{\partial \zeta} = -U'\Delta T \tag{9}$$

where

$$U' \equiv \frac{2UL}{\epsilon_o v_o r_i} \tag{10}$$

The stage model is obtained by writing the spatial derivatives appearing in the conservation equations in backward difference form. To simplify the equations we treat all heat capacities as constants. We further assume that the vapor phase is ideal and that the effect of composition on the vapor-phase density and velocity can be neglected, giving

$$v^* = \frac{T}{T_{\text{feed}}} \quad \rho_f = \rho_{fo}\frac{T_{\text{feed}}}{T} \tag{11,12}$$

where ρ_{fo} is the density of the hot inlet gas. We then obtain from Eqs. 8 and 9

$$\frac{dq_i}{d\tau} = \frac{1}{\rho_b \Delta\zeta}[(v^*c)_{i-1} - (v^*c)_i] \tag{13}$$

$$\frac{dT_i}{d\tau} = \frac{1}{\rho_b(c_s + c_a q_i)}\left\{\frac{\rho_{fo}c_f}{\Delta\zeta}(T_{i-1} - T_i) - \rho_b[c_a(T_i - T_{\text{ref}}) - \lambda_i]\frac{dq_i}{d\tau} - U'(T_i - T_{\text{amb}})\right\} \tag{14}$$

We have discussed elsewhere the manner in which equations similar to Eqs. 13 and 14 can be solved (Friday and LeVan, 1982). For the results presented here integration was carried out using the Gear's method package LSODE (Hindmarsh, 1980).

PHASE EQUILIBRIA

Along with the material and energy balances, the most important factor affecting the prediction of regeneration behavior is phase equilibria. The relationship between q, c, and T must be known accurately over wide ranges of concentration and temperature.

Apparatus

Figure 1 shows the apparatus used to measure isotherm data. The desired vapor-phase concentration was created by injecting n-octane, using a calibrated syringe pump, into a metered flow of nitrogen. The vapor was fed to a small adsorption column contained in a thermostat-controlled oven. The effluent was monitored with a gas chromatograph. The quantity of octane adsorbed was determined by weighing the adsorption column.

The adsorbent was type BPL granular carbon, manufactured

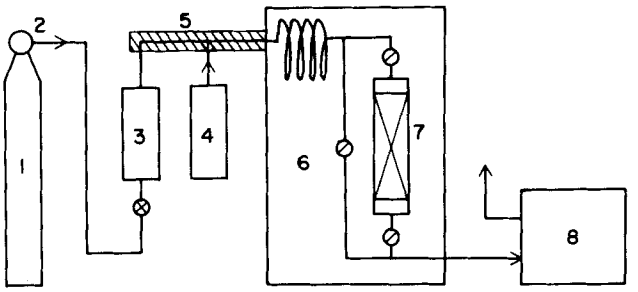

Figure 1. Apparatus for measurement of adsorption isotherm data.

1. Nitrogen cylinder
2. Regulator
3. Flowmeter
4. Syringe pump
5. Heating section
6. Oven
7. Adsorption bed
8. Gas chromatograph

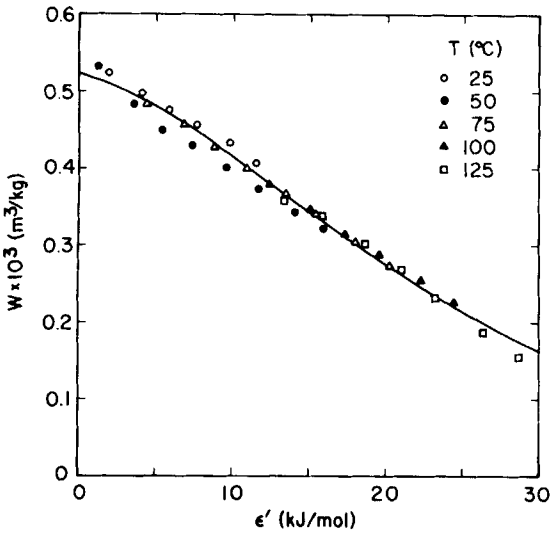

Figure 2. Isotherm data for *n*-octane adsorbed on type BPL granular carbon.

by Calgon Corporation for vapor-phase applications. Prior to the measurement of an isotherm, carbon was regenerated within the column using hot nitrogen to remove impurities. All data are on a weight-of-clean-carbon basis.

Isotherm Data and Correlation

Isotherms were measured at 25, 50, 75, 100, and 125°C. Hysteresis was examined and the results showed no measurable effect.

The most common methods for correlating phase-equilibria data for organics adsorbed on activated carbon are based on Polanyi-type pore filling models. W, filled pore volume per unit weight of adsorbent, is plotted versus ϵ', which is defined as

$$\epsilon' \equiv RT \ln(p_{sat}/p) \tag{15}$$

Data for all temperatures usually lie on a single curve, called the characteristic curve of the adsorbent. We adopted this approach and described our characteristic curve by the Dubinin-Astakhov (1971) equation, which is

$$W = W_o \exp[-(\epsilon'/\beta E)^n] \tag{16}$$

In calculating W, the density of the adsorbed phase was assumed to equal the density of saturated liquid at the isotherm temperature. p_{sat} was calculated from the Antoine equation

$$\log_{10} p_{sat} = A - \frac{B}{C + T} \quad \begin{matrix} p_{sat} \text{ in MPa} \\ T \text{ in K} \end{matrix} \tag{17}$$

with $A = 3.049$, $B = 1{,}355.1$, $C = -63.6$.

Our isotherm data are shown in Figure 2. The solid line is a plot of Eq. 16 with $W_o = 524$ cm³/kg, $\beta E = 27.1$ kJ/mol, $n = 1.45$, which were determined by minimizing differences between experimental and calculated values of ln W, using a least-squares criterion.

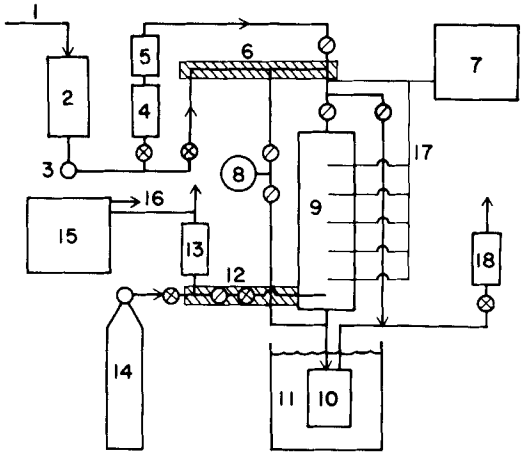

Figure 3. Apparatus for thermal regeneration experiments.

1. Air inlet
2. Filter
3. Regulator
4. Flowmeter
5. Saturator
6. Heating section
7. Multipoint recorder
8. Pressure gauge
9. Fixed-bed adsorber
10. Recovery vessel
11. Ice bath
12. Heated sample line
13. Flowmeter
14. Nitrogen cylinder
15. Gas chromatograph
16. Aspirator
17. Thermocouples
18. Flowmeter

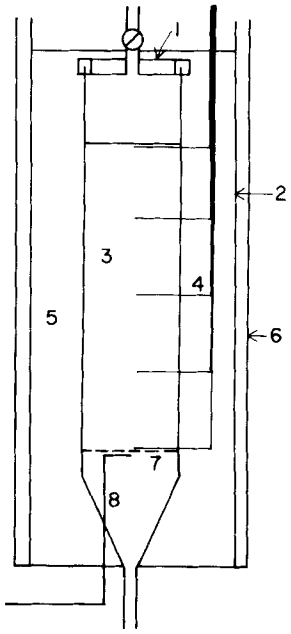

Figure 4. Details of bed design.

1. Plastic bushing
2. Foil lining
3. Carbon
4. Thermocouples
5. Insulation
6. Protection tube
7. Screen
8. Sample line

Heat of Desorption

Our formulation of material and energy balances sets forth a thermodynamic pathway in which adsorption and desorption take place at the reference temperature. This pathway requires that the heat of desorption be the isosteric heat of desorption, which is given with little approximation by the Clausius-Clapeyron equation

$$\lambda = -R \left.\frac{\partial(\ln p)}{\partial(1/T)}\right|_q \tag{18}$$

Thus, λ is obtained by solving Eq. 16 explicitly for p, then differentiating as indicated by Eq. 18. Equation 18 was also used to ob-

TABLE 1. REGENERATION EXPERIMENTS

Exp.	P MPa	ϕ	T_{feed} K	T_{init} K	T_{amb} K
1	0.20	1.0	373	296.5	296
2	0.20	0.1	373	296.5	297
3	0.20	0.01	373	298	296
4	0.20	1.0	343	295.5	295
5	0.11	1.0	373	297	296

tain the heat of vaporization of liquid octane by differentiating Eq. 17.

REGENERATION EXPERIMENTS

For a given set of physical properties, experimental results for thermal regeneration with hot purge gas can now be compared with predicted behavior. The apparatus used for the regeneration studies is shown in Figure 3. *n*-octane was adsorbed onto activated carbon at atmospheric pressure, then desorbed using hot air at atmospheric or higher pressure. The carbon was loaded with hydrocarbon at ambient temperature by passing into the bed a vapor of known concentration of *n*-octane in air. This vapor was created by mixing an air stream with a second air stream that had been sparged through three vessels containing the octane connected in series. The effluent from the bed was monitored using a gas chromatograph to make sure that saturation was complete.

For desorption the system was pressurized to the desired value and the flow rate of clean air was set. This air stream was initially shunted around the bed while it was heated to the desired feed temperature using a tube furnace and heating tape. The hot air stream was then fed to the bed. The propagation of thermal waves through the bed was monitored with thermocouples connected to a multipoint recorder. A small portion of the effluent was blended with nitrogen (1 part effluent to 3 parts nitrogen) to prevent octane from condensing in tubing at ambient temperature. Part of this vapor was drawn through the gas sampling valve of the chromatograph. Downstream of the bed, octane was removed from the exhaust in an ice bath to prevent any condensate from entering the main flow control valve and flowmeter.

Details of the bed design are shown in Figure 4. Efforts were made to keep heat capacities low and achieve close to adiabatic operation. The bed was made out of a copper tube (seam silver-soldered) with an inside diameter of 7.6 cm and a wall thickness of 0.05 cm. A Delrin (polyacetal plastic) bushing was used at the top of the bed for low heat capacity and structural strength. A brass funnel was used at the bottom of the bed to reduce the diameter gradually to nominally ½ in. (12.7 mm), the size of

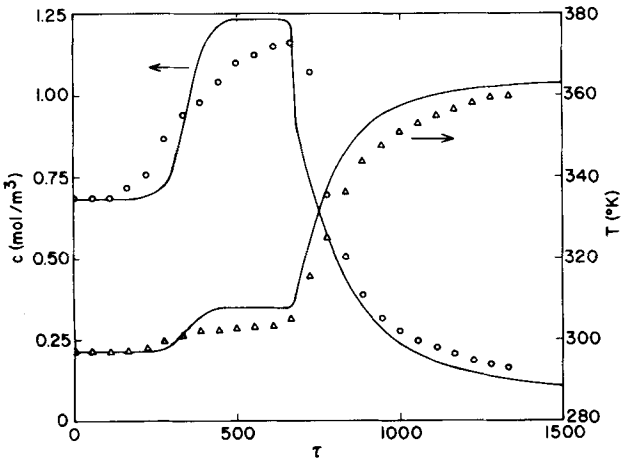

Figure 5. Breakthrough curves for Experiment 1.

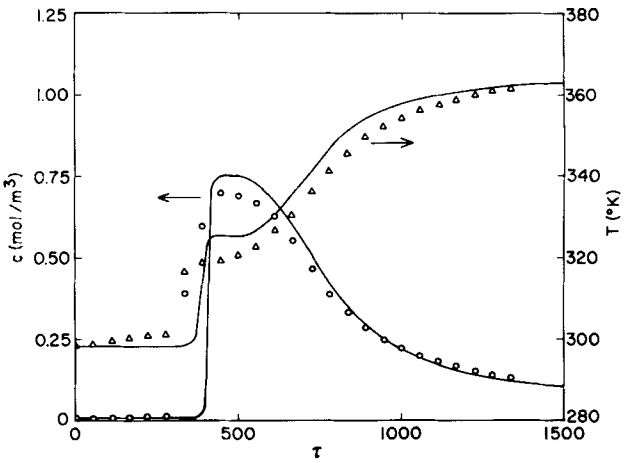

Figure 6. Breakthrough curves for Experiment 3.

main piping in the apparatus. A fine-mesh wire screen was used at the bottom of the packing to retain the carbon granules. Copper-constantan thermocouples were inserted into the bed every 20 cm by passing then through small brass sleeves silver-soldered to the copper tube and sealing them in the sleeves with epoxy. The lowest thermocouple in the bed was located just above the wire screen. The sample line to the gas chromatograph extended to just below the screen.

The bed was shielded by a pipe with an inside diameter of 16 cm. The annular space between the bed and the pipe was filled with silica aerogel (Syloid 244, Davison Chemical Div., W. R. Grace and Co.) for insulation.

The bed was packed to a depth of 80 cm with type BPL activated carbon granules that had been screened to 2.00 to 3.36 mm in size. Further details concerning apparatus design and operating procedures are contained in Friday (1983).

Determination of c_s and U

An exact solution to Eq. 9 for a thermal wave in the absence of adsorption can be obtained using Laplace transforms. For a bed initially at temperature T_{amb} we find at the bed outlet

$$\frac{T - T_{amb}}{T_{feed} - T_{amb}} = \exp\left(-\frac{U'}{\rho_{fo}c_f}\right) u\left(\tau - \frac{\rho_b c_s}{\rho_{fo}c_f}\right) \tag{19}$$

where u is the unit step function. Thus at a given time thermal breakthrough occurs, changing the temperature at the bed outlet from T_{amb} to another value which remains constant for larger times. This simple result was used to evaluate both c_s and U. The breakthrough time determines c_s. The final effluent temperature determines U.

Experiments were performed with clean carbon at various pressures, inlet temperatures, and flow rates to determine c_s and U. It was necessary to use dry gas to prevent adsorption of water vapor, which would affect the value determined for c_s. We obtained c_s = 1.70 kJ/kg·K, U = 0.0020 kJ/s·m²·K. The value of c_s, which includes contributions from the column wall, the top bushing, the piping, and the insulation, can be compared with the specific heat capacity of type BPL granular carbon, which Calgon gives as 1.05 kJ/kg·K.

RESULTS

Experiments were conducted for the five conditions shown in Table 1. Variations in regeneration pressure, feed temperature, and initial fractional saturation of the vapor phase were considered to examine their effects on regeneration behavior.

Additional parameters necessary to predict performance are

T_{ref} = 273 K

c_f = 1.06 kJ/kg·K

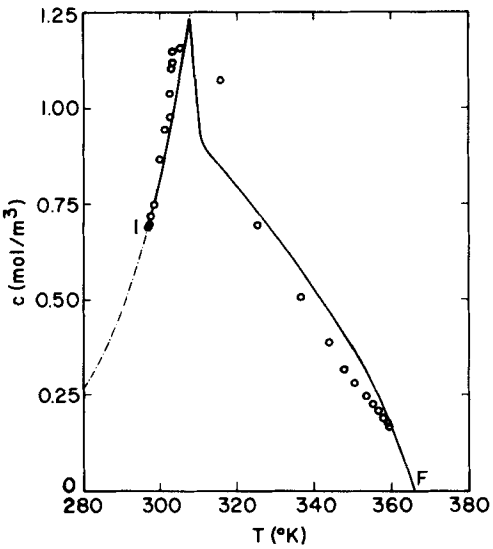

Figure 7. Regeneration path for Experiment 1.

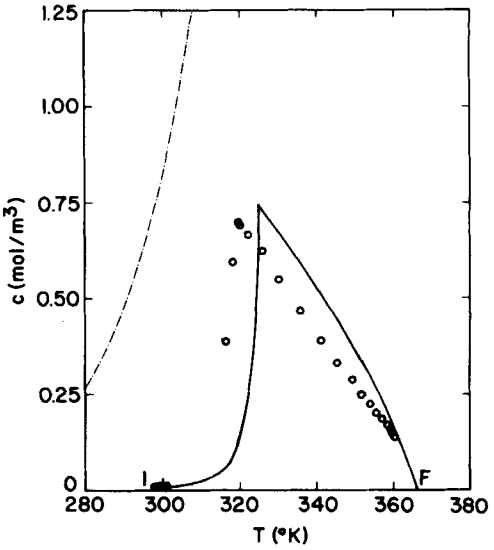

Figure 9. Regeneration path for Experiment 3.

ρ_b = 480 kg/m^3

c_a = 0.27 kJ/mol·K

w = 0.0032 kg/s

The mass flow rate of air was held constant for all experiments and corresponds to a volumetric flow rate of 163 L/min at STP. Superficial velocities at the bed inlet ranged from 0.37 to 0.67 m/s, depending on feed temperature and pressure.

Typical concentration and temperature breakthrough curves are shown in Figures 5 and 6 for experiments 1 and 3, respectively. In each case, two transitions are apparent, connected by a plateau. Solid lines indicate the predictions of the stage model using 30 stages, although any large number would have given reasonable agreement.

The nature of the regeneration process can be shown by plotting effluent fluid-phase concentration vs. effluent temperature. Such a plot for experiment 1 is shown in Figure 7. For this case the bed, fully saturated at ambient temperature was regenerated with air at 0.2 MPa and 373 K. The dashed curve shown in Figure 7 is the pure-component saturated vapor curve for n-octane calculated from Eq. 17. The initial condition of the bed is marked with an I and the final condition approached at the bed outlet is marked with an F. The solid line is a plot of the predicted regeneration path taken from Figure 5. Beginning at point I, since the vapor-phase concentration cannot exceed the saturation concentration to any appreciable extent, the data follow the saturated vapor curve to the plateau region (indicated by the high density of points taken at equal time intervals) near 305 K. The data then depart from the saturated vapor curve and approach a final effluent temperature of 365 K, which can be obtained from Eq. 19. The predicted behavior follows the general pattern of the experimental results, with the plateau at 308 K, where the predicted value of q exceeds the saturation capacity of the adsorbent by 13%.

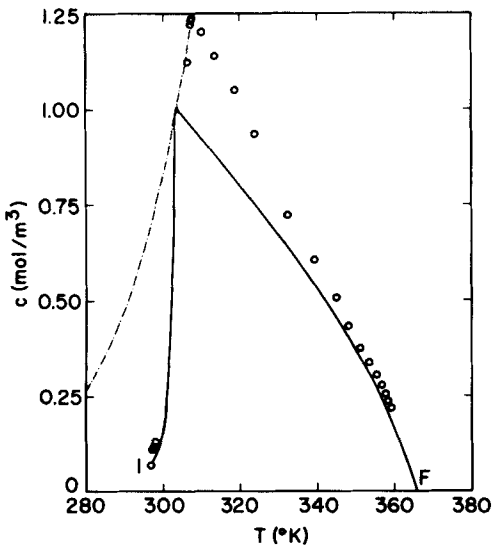

Figure 8. Regeneration path for Experiment 2.

Effects of initial saturation of the adsorbent are shown in Figures 8 and 9 for experiments 2 and 3, respectively. The beds, again regenerated with air at 0.2 MPa and 373 K, were initially in equilibrium with gas 10% and 1% saturated with n-octane at ambient temperature, corresponding to initial loadings of the adsorbent of 90 and 75% of the saturation capacity. For experiment 2 the saturated vapor curve is barely reached. A plateau temperature of 307 K was measured, whereas the model predicts 304 K with q exceeding the saturation capacity by only 0.2%. In experiment 3 the development of a saturated phase was neither found experimentally nor predicted by the model. At the highest fluid-phase concentration reached, q has increased to about 95% of the saturation capacity.

Figure 10 shows the effect of the reduced feed temperature used in experiment 4, where air at 0.2 MPa and 343 K was passed into a bed initially fully saturated with n-octane. Data points and the predicted regeneration path initially follow the saturated vapor curve from point I, as in experiment 1. The plateau temperature, however, is only 2 K greater than the initial bed temperature and the maximum value of q predicted is 2.8% greater than the saturation capacity. Leaving the plateau, a final bed temperature of 338 K is approached.

Results of experiment 5, in which the regeneration pressure was reduced to 0.11 MPa, are shown in Figure 11. The feed temperature was 373 K and the bed was initially fully saturated. Mea-

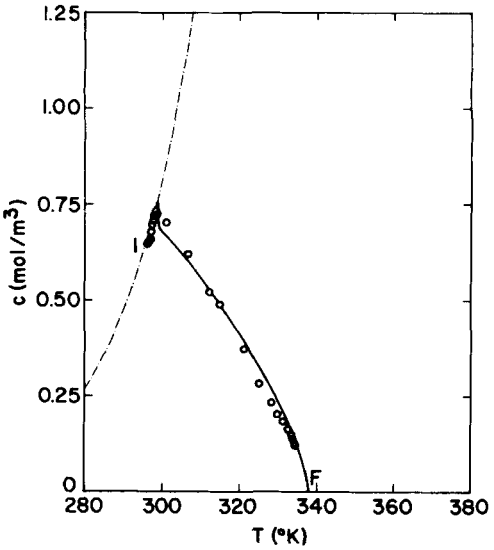

Figure 10. Regeneration path for Experiment 4.

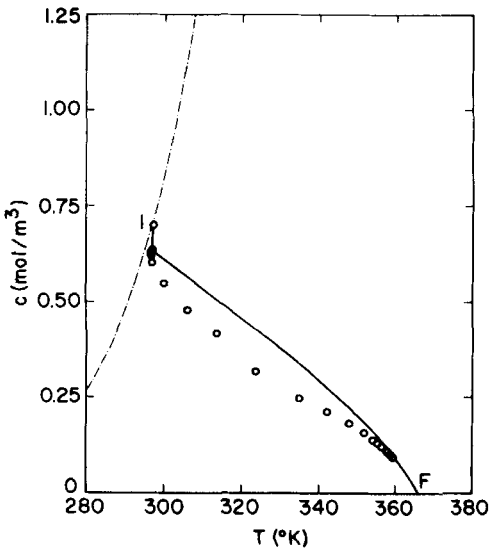

Figure 11. Regeneration path for Experiment 5.

surements and predictions are clearly different from those of previous cases. As soon as breakthrough begins, the solution path drops from the saturated vapor curve with a slight amount of cooling of the bed. Following the elution of the plateau, the final temperature of 365 K is approached. The largest value of q reached at any time is the initial value.

DISCUSSION

In three of the five experiments saturated vapor was eluted from the bed after the initial breakthrough, indicating the presence of liquid, most likely held in macropores, at the bed outlet. The results are consistent with our earlier predictions that an increase in initial loading, regeneration pressure, or feed temperature increases the likelihood that liquid will be formed.

The pairs of transitions shown in Figures 5 and 6 are qualitatively different, as indicated by both the experimental results and the model predictions. The first transition is much shallower in Figure 5 than in Figure 6, while the second transition is much sharper. A method of characteristics solution, restricted to adiabatic behavior, indicates that while the first transition in experiment 1 is abrupt, the solution for a gradual transition is almost physically acceptable. Also, the second transition in experiment 1 must be of combined form with an abrupt path taken from the saturated state (Friday, 1983; Friday and LeVan, 1984). For experiment 3 the first transition is strongly abrupt and the second transition is purely gradual.

Further insight into conditions for which the formation of a liquid phase can be expected can be obtained using Figures 7–11. Local equilibrium theory indicates that the path taken by the gradual part of the second transition should be completely independent of the path of the first transition. This can be seen in Figures 7–9 for regeneration using hot air at 0.2 MPa and 373 K. Furthermore, two possibilities exist for the path of a first transition leaving point I. Temperature, fluid-phase concentration, and stationary-phase concentration either all increase or all decrease. If all must increase to intersect at the plateau condition with the path of the second transition, as in Figures 7–10, then the value of q at the plateau will be the largest found and possibly exceed the saturation capacity of the adsorbent. Similarly, if T, c, and q all decrease leaving point I, as in Figure 11, then condensate cannot be formed. The path of the second transition and its relationship to point I is then the fundamental feature that determines whether or not it is possible for condensate to form.

In adopting the simple stage model we have chosen to focus our attention on the gross features of breakthrough curves, i.e., the locations and general shapes of transitions and the heights of plateaus. One approximation not related to the stage model has been introduced that affects these features. To simplify the analysis considerably, heat losses have been treated using a constant overall heat transfer coefficient and an effective stationary-phase heat capacity. In reality, radial temperature variations exist within the bed (creating radial concentration variations also) and some condensation may occur on the walls of the column. Furthermore, as the temperature waves propagate through the column heat losses can be expected to be somewhat greater than those predicted using an overall heat transfer coefficient evaluated at steady state (because temperature gradients within the insulation immediately adjacent to the column wall are larger for a given local bed temperature than the steady state gradient). Heat losses in the experiments were small, however, and measured and predicted plateau temperatures agree reasonably well, never differing by more than a few degrees. Also, the predicted plateau temperature is not sensitive to the number of stages, provided that the number of stages is large, and would not be changed by an analysis involving mass transfer resistances or particle-scale heat transfer resistances.

We close with a brief discussion of the full rate problem. In addition to heat losses, rate behavior can be expected to be influenced by both fluid mechanics and the transfer resistances. Variations of local void fraction, not only near the column wall but also well within the central core of the packing, lead to deviations from plug flow which contribute to the breadths of concentration waves at the bed outlet. In beds of large diameter the effects of this channeling become more pronounced because of the greater time (or axial distance) required for transverse diffusion and dispersion to damp out fluctuations of concentration over the cross-sectional area of the bed. Effects of flow maldistribution are well-documented in the chromatography literature, particularly concerning the decreased efficiency of columns of preparative size (e.g., Littlewood, 1962; Rijnders, 1966; Valentin, 1981). What data is available from studies on adsorption in beds of widely varying diameters show similar trends (LeVan and Vermeulen, 1984). In short, channeling should be expected to affect the performance of randomly packed adsorption beds in which concentration waves would otherwise be expected to be very sharp. This is most often the case

in gas-phase adsorption with very favorable equilibria.

The various mass and heat transfer processes can be compared to determine which mechanisms are likely to contribute to the detailed shapes of transitions. (This can be done only approximately, however. Surface diffusion coefficients are known to be strongly concentration-dependent. Furthermore, if a particle were to fill with liquid, then no intraparticle diffusion resistance would be present.) Using the formulas of Vermeulen et al. (1984) for mass transfer and adopting analogous relations for heat transfer, we find that the numbers of transfer units are of order 10^3 for axial dispersion of mass and energy (for which the number of transfer units can be shown to be equal to twice the number of stages), or order 10^2 for external mass and heat transfer, of order 10^2 for pore and surface diffusion acting in parallel, and of order 10^3 for intraparticle heat conduction. Thus it is likely that the specific shapes of transitions are influenced by external mass and heat transfer, intraparticle diffusion (principally surface diffusion), radial variations of temperature and concentration within the bed attributable to heat losses, and deviations from plug flow.

ACKNOWLEDGMENT

Acknowledgment is made to the Donors of The Petroleum Research Fund, administered by the American Chemical Society, for the support of this research.

NOTATION

c = gas-phase concentration of solute, mol/m^3
c_a = heat capacity of adsorbate and condensate, kJ/mol·K
c_f = heat capacity of gas phase, kJ/kg·K
c_s = effective heat capacity of adsorbate-free stationary phase, kJ/kg·K
E = activation energy, kJ/mol
h_f = enthalpy of gas phase, kJ/kg
h_s = enthalpy of stationary phase, kJ/kg
L = bed length, m
n = isotherm parameter
p = partial pressure of solute, MPa
p_{sat} = pure component vapor pressure of solute, MPa
P = total pressure, MPa
q = stationary-phase concentration, mol/kg
r_i = inside radius of bed, m
R = gas constant
t = time, s
T = temperature, K
T_{amb} = ambient temperature, K
T_{feed} = feed temperature, K
T_{init} = initial bed temperature, K
T_{ref} = reference temperature, K
U = overall heat transfer coefficient, kJ/s m^2·K
U' = modified overall heat transfer coefficient defined by Eq. 10, kJ/m^3·K
v = interstitial velocity, m/s
v^* = dimensionless flowrate
w = mass flowrate of air, kg/s
W = volume of adsorbate per unit weight of adsorbent, cm^3/kg
W_o = volume of adsorption space per unit weight of adsorbent, cm^3/kg
z = axial coordinate, m

Greek Letters

β = scaling factor
ϵ = void fraction of packing
ϵ' = isotherm parameter, kJ/mol
ζ = dimensionless axial coordinate
λ = latent heat of desorption or vaporization, kJ/mol
ρ_b = bulk density of packing, kg/m^3
ρ_f = density of gas phase, kg/m^3
τ = dimensionless time
ϕ = initial fractional saturation of vapor phase in bed
χ = porosity of particles

Subscripts

i = stage index
o = inlet condition

LITERATURE CITED

Basmadjian, D., K. D. Ha and D. P. Prouix, "Nonisothermal Desorption by Gas Purge of Single Solutes from Fixed-Bed Adsorbers. II: Experimental Verification of Equilibrium Theory," *Ind. Eng. Chem., Proc. Des. Dev.*, **14**, 340 (1975).

Basmadjian, D., "The Adsorption Drying of Gases and Liquids," *Advances in Drying*, A. S. Mujumdar, Ed., Hemisphere, New York, **3**, 307 (1984).

Dubinin, M. M., and V. A. Astakhov, "Development of Theories on the Volume Filling of Micropores During the Adsorption of Gases and Vapors by Microporous Adsorbents. 1: Carbon Adsorbents," *Izv. Akad. Nauk SSSR, Ser. Khim.*, **1**, 5 (1971).

Friday, D. K., and M. D. LeVan, "Solute Condensation in Adsorption Beds During Thermal Regeneration," *AIChE J.*, **28**, 86 (1982).

——, "Thermal Regeneration of Adsorption Beds. Equilibrium Theory for Solute Condensation," *AIChE J.*, **30**, 679 (1984).

Friday, D. K., "Purge Gas Regeneration of Adsorption Beds with Solute Condensation," Ph.D. Diss., Chem. Eng., Univ. Virginia (1983).

Hindmarsh, A. C., "LSODE and LSODI, Two New Initial-Value Ordinary Differential Equation Solvers," *ACM-SIGNUM Newsletter*, **15**(4), 10 (1980).

Jacob, P., and D. Tondeur, "Adsorption Nonisotherme de Gaz en Lit Fixe. III: Etude Experimental des Effets de Guillotine et de Focalisation Separation *n*-Pentane/iso-Pentane sur Tamis 5A," *Chem. Eng. J.*, **26**, 143 (1983).

LeVan, M. D., and T. Vermeulen, "Channeling and Bed-Diameter Effects in Fixed-Bed Adsorber Performance," *Adsorption and Ion Exchange—Progress and Future Prospects*, J. D. Sherman and T. Vermeulen, Eds., *AIChE Symp. Ser.* No. 233, **80**, 34 (1984).

Littlewood, A. B., *Gas Chromatography*, Academic Press, New York, 190 (1962).

Rijnders, G. W. A., "Preparative-Scale Chromatography," *Advances in Chromatography*, J. C. Giddings and R. A. Keller, Eds., Marcel Dekker, New York, **3**, 215 (1966).

Valentin, P., "Design and Optimization of Preparative Chromatographic Separations," *Percolation Processes: Theory and Applications*, A. E. Rodrigues and D. Tondeur, Eds., Sijthoff and Noordhoff, Alphen aan den Rijn, Netherlands, 141 (1981).

Vermeulen, T., et al., "Adsorption and Ion Exchange," *Chemical Engineers' Handbook*, 6th ed., McGraw-Hill, New York, Sec. 16 (1984).

Manuscript received May 4, 1984; revision received Oct. 24 and accepted Oct. 29, 1984.